Journal of Bioenergetics and Biomembranes, Vol. 32, No. 3, 2000

Three-Dimensional Structure of Nucleoside Diphosphate Kinase

Joël Janin,[1,5] Christian Dumas,[2] Solange Moréra,[1] Yingwu Xu,[3] Philippe Meyer,[1] Mohamed Chiadmi,[4] and Jacqueline Cherfils[1]

Received March 3, 2000; accepted May 12, 2000

Three-dimensional structures are known from X-ray studies of the nucleoside diphosphate (NDP) kinase of many organisms from bacteria to human. All NDP kinases have subunits of about 150 residues with a very similar fold based on the αβ sandwich or ferredoxin fold. This fold is found in many nucleotide or polynucleotide-binding proteins with no sequence relationship to NDP kinase. This common fold is augmented here with specific features: a surface α-helix hairpin, the Kpn loop, and the C-terminal extension. The α-helix hairpin and Kpn loop make up the nucleotide binding site, which is unique to NDP kinase and different from that of other kinases or ATPases. The Kpn loop and the C-terminal extension are also involved in the quaternary structure. Whereas all known eukaryotic NDP kinases, including mitochondral enzymes, are hexamers, some bacterial enzymes are tetramers. However, hexameric and tetrameric NDP kinases are built from the same dimer. The structural environment of the active histidine is identical in all. The nucleotide binding site is also fully conserved, except for a feature implicating C-terminal residues in the hexamer, but not in the tetramer. Structural data on the native and phosphorylated enzyme, complexes with substrates, inhibitor, and a transition state analog, give a solid basis to a mechanism of phosphate transfer in which the largest contributors to catalysis are the 3′-OH of the sugar and the bound Mg^{2+} in the nucleotide substrate. In contrast, we still lack structural data relating to DNA binding and other functions of NDP kinases.

KEY WORDS: Crystallography; ferredoxin fold; quaternary structure; nucleotide binding; transition state analog; substrate-assisted catalysis.

INTRODUCTION

The first three-dimensional structure of nucleoside diphosphate kinase (NDP kinase) to be determined by X-ray crystallography was the enzyme of the slime mold *Dictyostelium discoideum* (Dumas *et al.*, 1992). This initial study was followed by a series of others: the enzyme from the bacterium *Myxococcus xanthus* (Williams *et al.*, 1993), the Awd NDP kinase coded by the *abnormal wing disc* gene of *Drosophila melanogaster* (Biggs *et al.*, 1990; Chiadmi *et al.*, 1993), human NDP kinase B, product of the *Nm23*-H2 gene (Stahl *et al.*, 1991; Gilles *et al.*, 1991; Webb *et al.*, 1995; Moréra *et al.*, 1995a). More recently, a human mitochondrial NDP kinase (Milon *et al.*, 1997, 2000) and two isoforms of the enzyme from the bovine retina have also been examined (Ladner *et al.*, 1999). These X-ray structures and the corresponding entries in the Protein Data Bank are listed in Table I. They reveal

[1] Laboratoire d'Enzymologie et de Biochimie Structurales CNRS UPR9063, 91198-Gif-sur-Yvette, France.
[2] *Present address*: Centre de Biochimie Structurale, Faculté de Pharmacie, 15 avenue Charles Flahault, 34060-Montpellier 1, France.
[3] *Present address*: Biological Sciences, 701 Fairchild Center Columbia University, New York, New York 10027.
[4] *Present address:* Laboratoire de Cristallographie et RMN Biologiques Université René Descartes, 4 avenue de l'Observatoire, 75270-Paris 06.
[5] Author to whom all correspondence should be sent. email: janin@lebs.cnrs-gif.fr

0145-479X/00/0600-0215$18.00/0

Table I. NDP Kinase X-Ray Structures

Enzyme	Space group	Subunits per a.u*[a]	Resolution (Å)	Rfactor (%)[b]	PDB entry	Ref.[c]
Dictyostelium discoideum (slime mold)						
H122C mutant	$P6_322$	1	2.2	0.20	1ndk	a
Wild type	$P6_322$	1	1.8	0.20	1npk	b
Phosphorylated	$P6_322$	1	2.1	0.19	1nsp	c
+ TDP	R32	1	2.0	0.18	1ndp	d
+ ADP	R3	2	2.2	0.19	1ndc	e
+ ADP,AlF_3	$P3_121$	3	2.0	0.18	1kdn	f
+ ADP, BeF_3	$P3_121$	3	2.3	0.19	2bef	f
+ PAPS	$P3_121$	3	2.8	0.20	1bux	g
+ 3′-amino-3′-dADP	$P3_121$	3	2.6	0.23		h
+ 3′-fluoro-ddUDP	$P2_1$	6	2.7	0.21	1b99	i
+ α-borano-TDP	$P3_121$	3	1.9	0.23	1f6t	j
H122G + ADP	$P3_121$	3	2.5	0.20	1b4s	k
+ D4T triphosphate	$P3_121$	3	1.8	0.21	1f3f	j
N119A + AZT diphosphate	$P3_121$	3	2.3	0.22	1lwx	l
P100S	$P6_322$	1	2.6	0.19	1leo	m
P105G	$P6_322$	1	2.2	0.18	1ncl	n
Human						
Nm23-H2	$P2_12_12_1$	6	2.8	0.25	1nsk	o
+ GDP	$P2_12_12_1$	6	2.0	0.18	1nue	p
Nm23-H1						q
Nm23-H4	$P2_13$	2	2.4	0.18	1ehw	r
Rat						
NDP kinase α	$P6_122$	3	3.0	0.20		s
+ ADP	$P2_12_12_1$	6	2.2	0.22		s
+ GDP	$P2_12_12_1$	6	2.1	0.20		s
NDP kinase β	$P4_32_12$	3	3.0	0.22		s
Bovine retina						
Form A + GDP or cGMP	$P2_12_12_1$	6	2.4	0.20	1bhn	t
Form B + cGMP	$P4_32_12$	3	2.4	0.20	1be4	t
Drosophila melanogaster (Awd)						
No ligand	$P3_221$	3	2.4	0.17	1ndl	u
Phosphorylated	$P3_221$	3	2.2	0.18	1nsq	c
Saccharomyces cerevisiae (yeast)	$P2_12_12_1$	6	2.2	0.22		v
Myxococcus xanthus (bacterium)						
No ligand	$P4_32_12$	2	2.0	0.17	2nck	w
+ ADP	$P4_32_12$	2	2.0	0.23	1nlk	w
+ cAMP	$P4_32_12$	2	1.9	0.17	1nhk	x

[a] Whatever the space group and the number of subunits par asymmetric unit (a.u.) of the crystal form, the biological unit is a hexamer except for the tetrameric *Myxococcus* enzyme.

[b] The R factor measures the fit of the atomic model to diffracted intensities.

[c] References: (a) Dumas *et al.* (1992); (b) Moréra *et al.* (1994a); (c) Moréra *et al.* (1995a); (d) Cherfils *et al.* (1994); (e) Moréra *et al.* (1994b); (f) Xu *et al.* (1997a); (g) Schneider *et al.* (1998a); (h) Cervoni *et al.* (to be submitted); (i) Gonin *et al.* (1999); (j) Meyer *et al.* (2000); (k) Admiraal *et al.* (1999); (l)Xu *et al.* (1997b); (m) Karlsson *et al.* (1996); (n) Giartoso *et al.* (1996); (o) Webb *et al.* (1995); (p) Moréra *et al.* (1995b); (q) Min *et al.* (2000); (r) Milon *et al.* (2000); (s) Padmanabhan *et al.* (to be submitted); (t) Ladner *et. al.* (1999); (u) Chiadmi *et al.* (1993); (v) Chiadmi *et al.* (to be submitted), (w) Williams *et al.* (1993); (x) Strelkov *et al.* (1995).

that the 150-odd residues forming the polypeptide chain adopt a very similar fold in proteins from all origins. They confirm that NDP kinases are oligomeric: eukaryotic enzymes are homohexamers and the *Myxococcus* enzyme is a homotetramer. In addition, many X-ray studies were performed on point mutants or in the presence of ligands, substrates, or inhibitors. The structures of the mutants or complexes give a firm basis to the biochemical study of protein stability and of the catalytic mechanism of phosphate transfer. The design of new ligands, potential inhibitors of viral growth, is a by-product of this study. In contrast, the

structural analysis of other properties of NDP kinases such as DNA binding and cellular regulations (De la Rosa *et al.*, 1995; Okabe-Kado *et al.*, 1995; Postel, 1998) remains to be performed.

THE NDP KINASE SUBUNIT

The α/β Domain

A chain tracing of the NDP kinase subunit is shown in Fig. 1A for the *Drosophila* Awd protein. Except for specific features discussed below, the subunit fold is identical in NDP kinases from other origins. This should be expected for proteins whose sequence are 40% identical or more. For commodity, we use here the residue numbering in the human NDP kinase B (Nm23-H2) unless otherwise specified. The core of the subunit forms an α/β domain of about 90 residues, comprising a four-stranded antiparallel β-sheet and two connecting α-helixes, as in the schema of Fig. 1B. The remainder of the polypeptide chain, about 60 residues, is in additional features mentioned below. The topology of the β-sheet is defined by the strand order $\beta_2\beta_3\beta_1\beta_4$. Helixes α_1 and α_3 connect strands β_1 to β_2 and β_3 to β_4, respectively, and cover one face of the β-sheet, the bottom face in Fig. 1A. The β-sheet with its characteristic topology and the two connecting α-helixes, define a very common structural motif, which has been variously called αβ sandwich or βαββαβ fold, and also the ferredoxin fold, because it was first observed in *Pseudomonas aerogenes* ferredoxin (Adman *et al.*, 1973). The βαββαβ notation emphasizes that the fold comprises two βαβ units and has internal symmetry, but it should be noted that, in between the two parallel β-strands of each unit, there is a β-strand of the other unit running in the opposite direction. Thus, the βαβ units of a ferredoxin fold cannot fold separately.

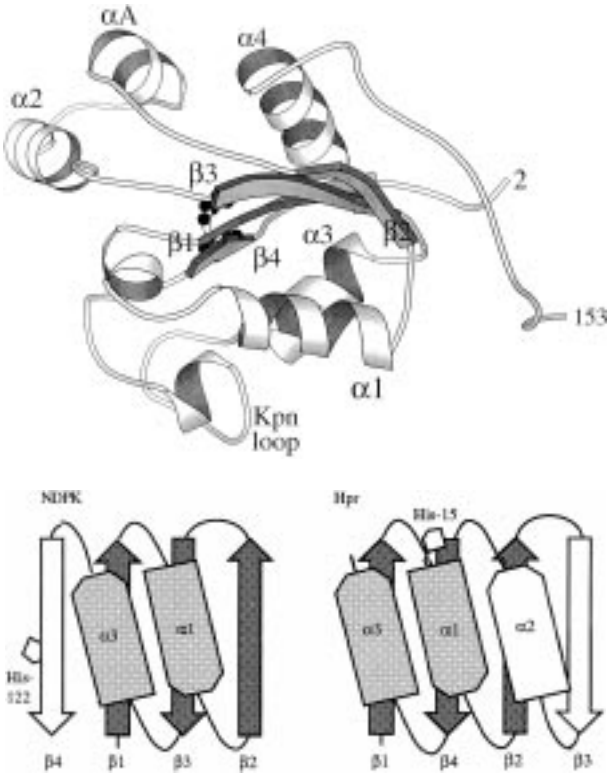

Fig. 1. The NDP kinase subunit. (A) Ribbon chain tracing of the subunit of the Awd NDP kinase of *Drosophila* (Chiadmi *et al.*, 1993). The active site histidine is in ball-and-stick. It is His-119 in *Drosophila*, which has one additional N-terminal residue compared to human NDP kinase B and His122 in *Dictyostelium*. Limits of structure elements are (NDP kinase B numbering): β_1 5–12, α_0 13–17, α_1 21–31, β_2 34–41, α_A 45–51, α_2 61–69, β_3 73–79, α_3 83–92, Kpn loop 96–116, β_4 117–120, α_4 123–133, C-terminal segment 134–152. (B) Topology diagrams of the NDP kinase and HPr folds. The ferredoxin fold found in NDP kinase is different from the HPr fold: the six secondary structure elements that characterize the fold occur in reverse order, with β_1 replacing β_4 and so on. Only the shaded part can be effectively aligned. The position of the phosphorylated histidines is indicated.

The packing of the α-helixes onto the β-sheet creates a hydrophobic core that is highly conserved in NDP kinases. Strands β_1 and β_3 in the middle of the sheet are the least variable parts of the sequence and very hydrophobic. Strand β_2, albeit an edge strand in the β-sheet, is buried as a result of dimer formation. It is also hydrophobic and effectively extends the hydrophobic core to the other subunit in the dimer. The sequence of strand β_2 is leucine-rich, especially in *Dictyostelium* where it has three leucines out of eight residues. These leucines form a "β-strand leucine zipper" which, while promoting dimerization, is completely unrelated to the α-helical dimerization domain of transcription factors. Amino acid substitutions in β_2 and elsewhere in the hydrophobic core are conservative with a remarkable exception: *Drosophila* has a proline (Pro76) half-way through strand β_3 and right at the center of the β-sheet. As proline lacks a peptide NH, a carbonyl group on neighboring strand β_2 is left unpaired (Chiadmi *et al.*, 1993). This ought to be highly destabilizing and distort the β-sheet structure, but the distorsion is purely local and the *Drosophila* protein is known to be stable to 70°C. This feature has no equivalent in other NDP kinases.

Similarity with Other Proteins

The ferredoxin fold observed in the NDP kinase subunit is a very common one in proteins. Table II lists "structural neighbors" where the geometry of the fold is particularly close to that of NDP kinase. The comparison is based on a superposition of the Cα atoms and yields a score measuring the degree of structural similarity. The score depends both on the number of Cα, which have been superimposed, and on their root-mean-square distance (RMSD). Taking human NDP kinase B as a reference, the similarity score is very high for other NDP kinases. Essentially all Cα atoms in the subunit can be superimposed with a RMSD of about 1 Å for eukaryotic enzymes and 1.5 Å for the bacterial enzyme. The score is much lower, but still statistically significant for other proteins in Table II. They contain 70 to 90 residues in four antiparallel β-strands and connecting α-helixes whose Cα superimpose onto their counterparts in NDP kinase with a RMSD of 3 to 4 Å. Table II shows that sequence identity is below 16%: none of the structural neighbors has significant homology to NDP kinase. The common ancestor, if there is one, must be very remote.

The ferredoxin fold is associated with all sorts of functions. Several proteins listed in Table II bind a (mono)nucleotide. For instance, the allosteric domain of the regulatory subunit of *E. coli* aspartate transcarbamylase, an early identified structural neighbor of NDP kinase (Dumas *et al.*, 1992), binds ATP, but it does so in an opposite orientation to NDP kinase (Moréra *et al.*, 1994b; Swindells and Alexandrov, 1994). Many others bind polynucleotides. A large family of RNA-binding proteins, examplified here by ribosomal protein S6, have the ferredoxin fold. DNA polymerases, which bind mono- as well as polynucleotides, also contain the fold in their so-called "palm" domain. Several of the proteins in Table II carry out phosphate transfer reactions. One is a ATP-dependent kinase like NDP kinase (hydroxymethyl-dihydropterin pyrophosphokinase; Xiao *et al.*, 1999), but it transfers a pyrophosphate, not a phosphate group, and yields AMP instead of ADP. Another is acylphosphatase (Pastore *et al.*, 1992), a small enzyme, which is often taken as a prototype ferredoxin fold.

HPr, a small protein component of the sugar transport and signal transduction pathway in bacteria, has a related fold, also with a four-stranded antiparallel β-

Table II. NDP Kinases and Their Structural Neighbors[a]

Protein	Score	RMSD (Å)	Aligned residues	Identity (%)	PDB entry
NDP kinases					
Nm23-H2		(0)	152	100	1nue
Drosophila	28	0.9	152	78	1nsq
Bovine retina	27	1.0	151	89	1be4
Dictyostelium	28	1.1	150	60	1kdn
Myxococcus	25	1.5	143	44	1nlk
Others					
Ribosomal protein S6	5.9	3.2	85	12	1ris
Phosphoglycerate dehydrogenase allosteric domain	5.3	2.9	72	11	1psd
Hydroxymethyl-dihydropterin pyrophosphokinase	4.8	2.9	89	16	1hka
Taq DNA polymerase palm domain	4.5	3.4	79	9	1taq
Elongation factor G	4.3	3.1	69	9	1dar
E. coli PII signal transduction protein	3.8	3.5	80	9	2pii
EBNA-1 nuclear protein	3.7	3.1	81	7	1b3t
Copper chaperone for superoxide dismutase	3.6	2.6	66	11	1qup
Aspartate transcarbamylase allosteric domain	3.5	3.0	71	11	8atc
Acylphosphatase	3.2	4.1	73	10	2acy
Subtilisin propeptide	3.0	2.7	58	14	1scj

[a] Structural similarity was estimated by the DALI procedure (Holm & Sander, 1993) with human NDP kinase B as the reference. Cα superpositions were performed on a set of structures representing the whole PDB and their result ranked according to the DALI Z score. The score depends on the root-mean-square distance (RMSD) of superimposed Cα and on their number, which is the number of aligned residues. A high score means that the structures are closely related. Fourty proteins (other than NDP kinases) had Z scores above 2.0. "Identity" to the NDP kinase B sequence is derived from the alignment based on the Cα superposition.

sheet and two connecting α-helixes. Like NDP kinase, HPr is phosphorylated on a histidine, so an evolutionary relationship could be considered. However, Fig. 1B shows that the HPr topology is distinct from that of NDP kinase or any of the proteins listed in Table II. The same elements of secondary structure are present in reverse order, which cannot be achieved by divergent evolution (Herzberg *et al.*, 1992; Swindells *et al.*, 1993; Janin, 1993). The more likely explanation is convergence toward a simple, stable structure, and this probably also applies to instances of the ferredoxin fold in proteins with unrelated sequence and function.

The Helix Hairpin, Kpn Loop, and C-Terminal Segment

In most proteins with a ferredoxin fold, the central β-sheet has one face covered by the two connecting α-helixes, and the other face open. RNA-binding proteins and the palm domain of DNA polymerases bind RNA or DNA on the open face. In NDP kinase, both faces are covered, the lower face by α_1 and α_3 and the upper face by structural elements added to the ferredoxin fold: a pair of helixes labeled α_A-α_2 that forms a hairpin inserted between strands β_2 and β_3 and helix α_4, which follows strand β_4. Strand β_4, which carries the active site histidine, is on the edge of the β-sheet and remains partly accessible.

Two additional features, the Kpn loop and the C-terminal segment complete the NDP kinase subunit fold. The 22-residue Kpn loop comprises residues 96–117 in NDP kinase B and is located between α_3 and β_4. Pro97 of Awd, replaced with Ser in a *Drosophila* mutant called *kpn* (*Killer-of-prune*) (Lascu *et al.*, 1992), is the first residue of this loop. Thus, the loop was named by us after the mutant. The Kpn loop is a small compact structure in which are summarized all types of helical structures: it has a turn of 3_{10} helix, a turn of polyproline II left-handed helix, and a turn of a standard α-helix. The latter effectively extends helix α_3 by one turn.

The C-terminal segment extends beyond helix α_4 and comprises the last 20-odd residues (134–152 in NDP kinase B) of hexameric eukaryotic NDP kinases. In the hexamer, the C-terminus of each chain interacts with a neighboring subunit. In *Myxococcus* and in other tetrameric bacterial NDP kinases, the C-terminal segment is shorter (10–12 residues) and not implicated in the quaternary structure. Albeit hexameric, the *Dictyostelium* enzyme also shows peculiarities. The sequence of its last 13 residues is highly divergent and contains a single-residue gap. The conformation of this part of the polypeptide chain differs from the one observed in Awd or NDP kinase B, deviating by up to 6 Å from the other chain tracings a few residues from the end. Yet, it recovers its path and the conserved C-terminal Tyr–Glu dipeptide is at the same position in all three proteins.

Variable and Mobile Parts

The N-terminus of the polypeptide chain, the α_A-α_2 hairpin, and the C-terminal segment are the most divergent parts of the NDP kinase sequence. These three regions are also the most mobile in the three-dimensional structure. In X-ray data, one criterion for mobility is the spread of the electron density shown in atomic coordinate files by the value of atomic temperature factors (B factors). B factors are less than 30 $Å^2$ in well-ordered regions, which implies that atoms remain within 0.6 Å root-mean-square of their mean position. Most main chain atoms in the crystal structures listed in Table I follow this rule. Disordered regions have larger B factors, up to 80 $Å^2$. In extreme cases, no electron density is seen and the corresponding residues are missing altogether from the atomic coordinate file. *Dictyostelium* has four additional residues at the N-terminus compared to most other NDP kinase sequences. These residues are present in the crystal, but they are fully disordered and the files begin with residue 5 or 6, where the other sequences start. The same applies to the C-terminus of the mitochondrial Nm23-H4 protein, where the sequence indicates the presence of additional residues. Twelve residues of the C-terminal segment are fully disordered in the crystal (Milon *et al.*, 2000).

In most NDP kinase X-ray structures, the C-terminal segment and the α_A-α_2 hairpin are relatively mobile, although they can be located in the electron density. Atoms in these regions have high B factors and their position changes from one crystal structure to another, or even between subunits in crystal forms that have more than one subunit in the asymmetric unit. In the latter case, the polypeptide chain usually superimposes to better than 0.3 Å over most of its length. This is close to the experimental error of the atomic positions, about 0.2 Å for main chain atoms at 2 Å resolution. Thus, the subunits have identical conformation except in the α_A-α_2 hairpin and the C-terminal segment, which may move by 1–2 Å. Such

local conformation changes may, in part, result from crystal-packing interactions between protein molecules, which are different between crystal forms and between subunits within an asymmetric unit. In addition, a 2 Å global movement affects the α_A-α_2 hairpin in relation to nucleotide binding. In X-ray data taken in the absence of a ligand, the hairpin has high B factors indicating mobility. In the presence of a ligand, the hairpin locks onto the bound nucleotide, and its B factors drop.

In crystals, the mobility of the hairpin is certainly limited by the crystal packing and one could imagine that much larger movements take place in solution. We checked this possibility by taking proton NMR data. The slow rotational diffusion of a 100 kDa molecule makes the resonance spectra very broad and no resolved peaks are expected unless some parts rotate much faster than the bulk. Sharp proton resonances were observed in 500-MHz proton spectra of *Dictyostelium*, but not NDP kinase B. All could be attributed to the disordered N-terminal residues (Xu *et al.*, 1997c) suggesting that atomic mobility is not very different in solution and in the crystals.

Fig. 2. Hexameric human NDP kinase B. The hexamer is viewed along its threefold axis, with the twofold axes in the plane of the figure. The Kpn loops are at the center near the threefold axis. Within each of the three dimers, there is a single β-sheet extending from the front to the back subunit. The bound GDP molecules are drawn as Van der Waals spheres, with the guanine bases pointing out of the protein. Adapted from Moréra *et al.* (1995b).

THE QUATERNARY STRUCTURE

NDP kinases exist in two different quaternary structures. All known eukaryotic enzymes are hexamers, even the mitochondrial Nm23-H4 form; some bacterial enzymes are tetramers, as in *Myxococcus*. The hexamer, illustrated in Fig. 2, is a compact disk about 70 Å in diameter and 50 Å thick. It has dihedral D3 symmetry and can be viewed as comprising two trimers related by twofold symmetry, or three dimers related by threefold symmetry. The tetramer is about 60 Å in all dimensions; it has D2 symmetry and is composed of a pair of dimers. Remarkably, these dimers are like those of the hexamer, indicating that the two types of quaternary structures use the same set of contacts between subunits to build a dimer, and pointing to the dimer as a likely intermediate in the assembly of both the tetramer and the hexamer.

The Dimer Interface

NDP kinase subunits dimerize by β-sheet extension: subunits sit side by side with their central β-sheets effectively forming a single, eight-stranded, antiparallel β-sheet. Two main–chain to main–chain hydrogen bonds link strand β_2 of one subunit to its counterpart in the other subunit. This mode of dimerization is frequent in oligomeric proteins with an α/β fold. In animal NDP kinases and *Myxococcus*, the dimer interface involves 20 to 25 residues and buries approximately 1050 $Å^2$ on each subunit, or 14% of its total surface area accessible to solvent. These are typical values for subunit interfaces in oligomeric proteins (Janin *et al.*, 1988). The dimer interface is significantly smaller (640 $Å^2$ and 18 residues) in *Dictyostelium* NDP kinase, where the C-terminal segment contributes less to it.

The residues making dimer contacts belong to helix α1, strand β_2, and the 140–145 stretch of the C-terminal segment. While the dimer interface is conserved as a whole from *Myxococcus* to human, remarkably few contact residues are invariant throughout the range of known sequences. For instance, Phe39 and Tyr142, which are major contributors to the dimer interface in animal NDP kinases, are, respectively, a glutamine and a glutamate in *Dictyostelium*. One key residue, Glu29, is nevertheless invariant. Its carboxylate receives two hydrogen bonds from main chain amino groups across the dimer interface and these hydrogen bonds are fully conserved, like those linking the two strands β_2 in the β-sheet. In animal NDP

kinases, two additional hydrogen bonds involve the Gln17 side chain. One exists in *Myxococcus*, where the equivalent residue is Glu, but not in *Dictyostelium*, where it is Ala. The total number of hydrogen bonds per dimer interface is 10 to 12, each duplicated by symmetry. The contribution of these interactions to the stability of the assembly remains to be tested by site-directed mutagenesis.

The Tetramer and Hexamer Interfaces

The tetramer interface seen in *Myxococcus* NDP kinase is comparatively small, burying 470 $Å^2$ on each subunit and involving only 13 residues from strand β_2, helix α_A, the end of helix α_4, and the first part of the C-terminal fragment. These residues are mostly polar and, in the absence of a sizable hydrophobic interface, the tetramer may easily dissociate. Equivalent residues in eukaryotic NDP kinases are accessible on the protein surface.

An entirely different set of contacts is used to assemble dimers into a hexamer. Interfaces within trimers are larger than within dimers and less polar, the number of hydrogen bonds being approximately the same (10–12). In *Drosophila*, each subunit loses 1700 $Å^2$, or 20% of its accessible surface area, in trimer contacts. Forty residues, representing more than one-quarter of the polypeptide chain, make these contacts. The number is about the same in NDP kinase B and 15% less in *Dictyostelium*. In all three proteins, the most important polar side chains at the trimer interface are those of Arg18 and Lys31. They donate hydrogen bonds to main chain carbonyl groups of the neighboring subunit and they are invariant in eukaryotes. Arg114 in animals and Lys85(81) in *Dictyostelium*, also donate hydrogen bonds, but the latter residue is a leucine in most animal sequences. Another hydrogen bond between the NH of Glu-152 and the side chain of residue 111 is conserved. Residue 111 can be Glu, Gln or Asp; Glu152 is the C-terminal residue of the chain.

The largest contributors to the trimer interface are the Kpn loop and C-terminal residues 149–152. The Kpn loop alone accounts for nearly one-half of the interface area. The tip of the loop is near the threefold axis of the hexamer. Three Kpn loops come together on the top face and three on the bottom face of the disk-shaped protein molecule. They enclose a large central cavity filled with about 100 water molecules, many of which show as resolved peaks in the electron density of *Dictyostelium* NDP kinase at 1.8 Å resolution. In contrast, the *Myxococcus* tetramer has no central cavity and its Kpn loops are completely accessible on the protein surface. Nevertheless, the loop conformation is essentially the same as in the hexamer. Therefore, the extensive subunit interactions seen in eukaryotic NDP kinases have little effect on the subunit fold, although they play a major part in the thermodynamic stability, as the site-directed mutagenesis of individual contact residues has demonstrated.

The Kpn Mutation Affects Subunit Contacts

The *kpn* mutation of the *Awd* gene substitutes a serine for Pro96 (NDP kinase B numbering). While the *Drosophila* mutant protein has not been studied directly by crystallography, the mutation was reproduced by site-directed mutagenesis in *Dictyostelium*, and the mitochondrial Nm23-H4 enzyme has a serine (Ser129) at the equivalent position. X-rays structures are available for the P100S *Dictyostelium* mutant and for Nm23-H4 (Karlsson *et al.*, 1996; Milon *et al.*, 2000). The structural consequences of the Pro->Ser substitution can be derived by comparing the P100S mutant to the wild-type *Dictyostelium* protein, or by comparing Nm23-H4 to Nm23-H2. The same conclusions are drawn in either case. The substitution introduces two new hydrogen bond donor groups, the NH and OH of the serine. They find the main chain carbonyl of residue 111 as a hydrogen bond partner, forcing the 111–112 peptide bond to flip 180°. Residue 111 is part of the trimer interface and implicated in an interaction with the NH of the C-terminal glutamate of a neighboring subunit. This interaction is disrupted in the P100S mutant and also in Nm23-H4, where C-terminal residues are disordered. Thus, the Kpn mutation appears to destabilize subunit interaction within trimers, in accordance with the large effect on protein stability, which is seen in *Drosophila*, in the *Dictyostelium* mutant, and in Nm23-H4 (Lascu *et al.*, 1992; Karlsson *et al.*, 1996; Milon *et al.*, 2000). It does so indirectly, by inducing a local conformation change and modifying the network of hydrogen bonds that connects position 96 to the C-terminus of a neighboring subunit. This in contrast with the P105G mutation of the *Dictyostelium* enzyme, which affects a residue directly located at the interface. It has a similar effect on protein stability, yet it induces no observable conformational changes (Giartoso *et al.*, 1996).

THE ACTIVE SITE

The NDP kinase active site comprises the nucleophilic histidine (His-118 in NDP kinase B) and the nucleotide binding site. There is a single binding site per subunit which accepts two types of substrates, the nucleoside triphosphate that donates and the nucleoside diphosphate that receives the phosphate group. The binding site forms a cleft on the protein surface, about 20 Å long, 6 Å wide, and 10 Å deep. His118 is at the bottom of the cleft. NDP kinase binds a nucleotide in an entirely different way from the "classic" mode seen in protein kinases, in nucleoside monophosphate kinases such as adenylate kinase, or in ATPases and GTPases (Schulz, 1992). Its mode of binding appears to be unique at present (Kinoshita *et al.*,1999).

The NDP kinase active sites are identical and independent within a tetramer or hexamer. They are also structurally identical in different enzymes and almost all the residues involved in the active site are fully invariant from bacteria to man. Their role in catalysis, extensively tested by site-directed mutagenesis in *Dictyostelium*, can safely be extended to the enzymes from other sources. In addition, a major conclusion of both the structural and the biochemical data is that critical interactions for catalysis are made not with protein groups, but with the 3′-OH of the sugar and the bound metal ion, that is, within the substrate itself.

The Catalytic Histidine and Phosphohistidine

His118 is in the middle of the very short (four residues) strand β_4, which immediately follows the Kpn loop. The connection between the loop and the β-strand is a sharp turn with a conformation that requires residue 116 to have a positive ϕ angle. In most eukaryotic NDP kinases, 116 is an isoleucine, which is remarkable, for the branched side chain makes the positive ϕ value especially unfavorable. If instead, Ile116 had a β-strand conformation, its side chain would be in contact with that of His118 and block access of the incoming nucleotide substrate to the imidazole group. The unusual main chain conformation of residue 116 is found in all NDP kinase structures. It is maintained by a hydrogen bond from the NH of Ile116 to the side chain of Asp14, a conserved residue in most sequences. In *E. coli*, Asp14 is replaced with an asparagine that can make the same interaction.

In contrast to Ilel16, the catalytic histidine has a standard main chain and side-chain conformation for a β-strand residue. The N_ϵ atom of its imidazole group interacts with the carboxylate of Glu129 on helix α_4, whereas N_δ is free (Fig. 3). The invariant glutamate also interacts with the hydroxyl group of Ser120, down two residues from His118 on strand β_4. The resulting His–Glu–Ser triad may recall the Ser–His–Asp triad of serine proteases. However, in trypsin and related proteases, Ser is a nucleophile and His a catalytic base. In NDP kinase, His118 is a nucleophile and Glu129 could conceivably act as a base, although the mechanism requires no proton transfer. The E129Q mutant retains 0.5% activity, which makes it unlikely that the glutamate is a base (Tepper *et al.*, 1994). Moreover, substitution of Ser120 has only a minor effect on catalysis. The role of Glu129 must be to keep the imidazole group in the proper position and orientation, and also to keep N_ε protonated. At neutral pH and above, this guarantees that N_δ remains unprotonated and ready to perform a nucleophilic attack on the incoming substrate.

X-ray structures of the phosphorylated form of *Drosophila* and *Dictyostelium* NDP kinases are available (Moréra *et al.*, 1995a). They show remarkably little change in the protein, even in the immediate environment of the phosphohistidine. Because the derivative is not stable over the period of a few days required for crystallization, phosphorylation had to be performed on the crystalline enzyme. We were unable to do that sim-

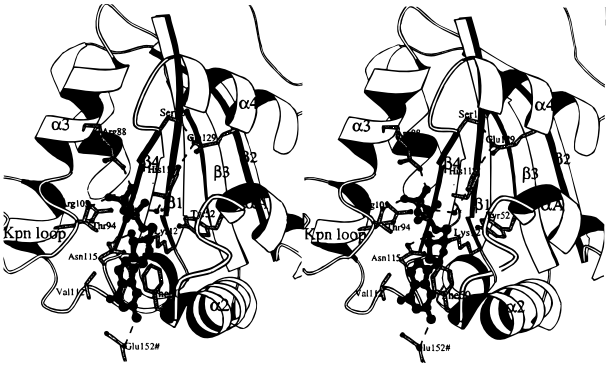

Fig. 3. The nucleotide-binding site. Stereo view of the human NDP kinase B subunit displaying the bound GDP molecule in black bonds and protein side chains that interact with it in grey. The active site His118 at the center interacts with the Glu129 side chain, itself bonded to Ser120. A water molecule (black dot) links the His118 side chain to the β-phosphate of GDP. At the bottom of the figure, the side chain of Glu152 interacts with the -NH_2 group on the guanine base; Glu-152 is the C-terminal residue of an adjacent subunit and this interaction can only be made in a hexamer. Adapted from Moréra *et al.* (1995b).

ply by adding ATP or another nucleoside triphosphate. Binding (or exchanging) the nucleotide requires a movement of the α_A-α_2 hairpin which, albeit small, appears to be forbidden by the crystal packing. Thus, a small molecule, phosphoramidate ($NH_2PO_3H^-$), was used as a phosphate donor and diffused into the crystal. The electron density shows that it specifically labels the N_δ position of the active site histidine, leaving untouched all other histidines or potential phosphate acceptors. Moreover, a [^{31}P] NMR study of NDP kinase phosphorylation in solution shows that the product is the same with phosphoramidate as with ATP, although the reaction is several orders of magnitude slower (Lecroisey *et al.*, 1995). In the X-ray structure, the phosphohistidine hydrogen bonds with the phenolic oxygen of Tyr52. It makes no other direct interaction with the protein, but water molecules bridge it to the guanidinium groups of Arg88 and Arg105.

The Base and Sugar Moieties

The NDP kinase substrate binding site accepts both a ribose and a 2′-deoxyribose and all common nucleobases. X-ray structures of complexes with ADP, TDP, and GDP (Williams *et al.*, 1993; Moréra *et al.*, 1994, 1995; Cherfils *et al.*, 1994) show the bound nucleotide located between the α_A-α_2 hairpin and the Kpn loop. The base is near the protein surface; the phosphate groups, more deeply buried, point toward the catalytic histidine. In nucleotide-free NDP kinase, the empty cleft is about 2 Å wider than in the complexes. The substrate must enter the cleft with the negatively charged di- or -triphosphate moiety first. Several basic residues line the cleft, creating a positive surface potential, which helps the substrate in. Once in position, a movement of the α_A-α_2 hairpin locks the cleft on the nucleotide.

Figure 3 details the mode of binding of GDP to human NDP kinase B (Moréra *et al.*, 1995). The guanine base is sandwiched between Val-112 and the phenyl group of Phe60 onto which it stacks. Val112 belongs to the Kpn loop; Phe60, located at the tip of the α_A-α_2 hairpin, is an invariant residue, yet it can be substituted by tryptophan with no loss of affinity (Schneider *et al.*, 1998b). Adenine in ADP and thymine in TDP bind in the same way as guanine. A comparison of the various complexes shows that the base can shift by 3–4 Å in its plane, suggesting that the cleft is designed to fit any planar aromatic group. The polar groups play only a minor part. Guanine carries five, yet only one polar interaction is made: its N2 amino group is within hydrogen-bonding distance of the δ-carboxylate of the C-terminal Glu 152 of another subunit in the hexamer. Whereas the C-terminal segment of each polypeptide chain extends up to the mouth of the binding cleft of a neighboring subunit within the same trimer, such an interaction cannot exist in *Myxococcus* and other tetrameric NDP kinases with short C-terminal segments. It also appears to be guanine specific, for other common nucleobases either have no substituent on C2 (adenine), or it is too far for a hydrogen bond (pyrimidines). Instead, water-mediated interactions are observed between the Glu152 δ-carboxylate and polar groups of the adenine or thymine base in ADP and TDP complexes.

Unlike the polar groups of the base, the sugar is buried and makes many polar interactions. In ribose, both the 2′-and the 3′-OH are within hydrogen-bonding distance of the amino group of Lys12 and of the amide group of Asn115. These residues are invariant and Lys12 is also implicated in catalysis. Its substitution severely hampers activity (Tepper *et al.*, 1994), whereas Asn-115 can be replaced (*Xu et al.*, 1997b). In deoxyribose, a water molecule can replace the missing 2′-OH (Cherfils *et al.*, 1994), apparently with little loss of binding energy. Either sugar adopts a C3′-*endo* ring pucker with the base in *anti* position. This applies to the natural substrates ADP, TDP, or GDP, which have essentially the same mode of binding. Nevertheless, the binding cleft can accept other sugar conformations. Inhibitors such as 3′,5′-cyclicAMP or -GMP (cAMP/cGMP), 3′-azido-thymidine (AZT) diphosphate or 3′-phosphoadenosine-5′-phosphosulfate (PAPS), occupy the same site as the substrates. These compounds all have different geometries, yet they all bind with the base and at least one phosphate in the same position as for a normal substrate, thanks in part to their different sugar pucker (Strelkov *et al.*, 1995; Ladner *et al.*, 1999; Xu *et al.*, 1997; Schneider *et al.*, 1998a).

The Phosphate Groups and Metal Ion

The crystalline complexes with ADP, GDP, and TDP also display interactions made by the phosphate groups. NDP kinase has no equivalent to the P-loop present in many ATP- or GTP-binding proteins (Schulz, 1992). The protein groups involved are not main chain NH groups as in a P-loop, but the side chains of Lys-12, Tyr52, Arg88, Thr94, and Arg105, all

invariant residues whose substitution by site-directed mutagenesis reduces activity at least ten fold. The α-phosphate remains accessible to solvent and interacts only with Thr94. In *Myxococcus* and *Dictyostelium*, His55 (NDP kinase B numbering) is also involved, but this residue is a leucine in animal sequences. The β-phosphate is located more deeply inside the protein in contact with Thr94, Arg88, and Arg-105.

The binding mode of the γ-phosphate is less obvious. Attempts to diffuse or cocrystallize ATP with the enzyme leads to a mixture of species including ADP and to uninterpretable density. A mutant NDP kinase lacking the catalytic histidine, cocrystallizes with ATP, yielding the hydrolysis products ADP and P_1 which remain bound to the protein (Admiraal *et al.*, 1999). With the wild type, the best available model is the ADP-beryllium fluoride complex (Xu *et al.*, 1997a). In the complex, the BeF_3^- ion is located halfway between the β-phosphate of ADP and N_δ of His118, where the γ-phosphate should be expected to be. BeF_3^- is a tetrahedral species resembling a normal phosphate group. The three fluoride ions, which mimick phosphate oxygens, interact with the Lys12, Tyr52, and Arg88 side chains and also with the main chain NH of Gly119. Beryllium fluoride can be replaced by aluminium fluoride, binding at the same location as the AlF_3 species (Fig. 4). AlF_3 is planar and trigonal like a γ-phosphate undergoing transfer with inversion. Thus, ADP–BeF_3 reproduces the geometry of ATP in the Michaelis complex and ADP–AlF_3 reproduces the transition state of the reaction (Xu *et al.*, 1997a). Surprisingly, neither compound is a strong inhibitor of NDP kinase activity in standard enzymic assays.

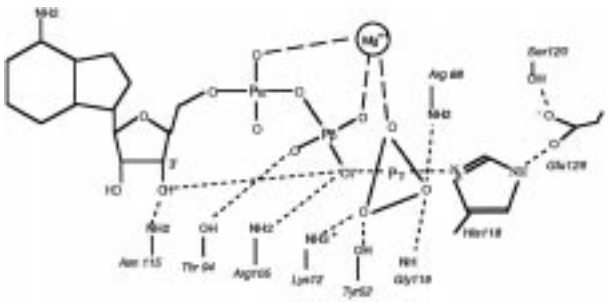

Fig. 4. A model of the transition state in the phosphate transfer reaction. The γ-phosphate of ATP is undergoing transfer from the β-phosphate onto nitrogen N_δ of His118. In the transition state, it takes up the geometry of a trigonal bipyramid, with the leaving group (O_7) and attacking group (N_δ) in apical position. Partial bonds from P_γ to these two atoms are indicates by dashed lines. A hydrogen bond (short dashes) from the sugar 3′-OH activates O_7. The negative charge on the three equatorial oxygens as neutralized by Mg^{2+}, Lys-12, and Arg88. Additional interactions involve Tyr-52 and the main chain NH of Gly119. The geometry and pattern of interactions depicted here is that of AlF_3 in the ADP–AlF_3 complex, which mimicks the transition state (Xu *et al.*, 1997b).

The conformation of the bound nucleotide allows the β-phosphate to fold back toward the sugar and hydrogen bond with its 3′-OH group. This bond is specific to NDP kinase and cannot form in other ATP-dependent kinases or in NTPases, where the ribose phosphate moiety usually adopts an open conformation (Moodie and Thornton, 1993). The bond is to the oxygen atom, which bridges the β- and γ-phosphate of a nucleoside triphosphate (NTP). This oxygen is the leaving group when NTP phosphorylates His118 and, by virtue of microreversibility, the attacking group when NDP dephosphorylates the histidine. The bond to the 3′-OH makes the bridging oxygen more reactive. Its catalytic importance is emphasized by the very low activity of NDP kinase on 3–deoxy-and 2′, 3′-dideoxynucleotides. Analogs where the 3′-OH is missing or replaced by a group that cannot donate a hydrogen bond, are phosphorylated 10^4 to 10^5 times less efficiently than normal substrates (Bourdais *et al.*, 1996; Schneider *et al.*, 1998b; Gonin *et al.*, 1999). Thus, deleting the 3′-OH cripples catalysis orders of magnitude more than deleting any protein group except the His118 imidazole. This observation is of great pharmacological significance, for nearly all drugs targeted against the reverse transcriptase of HIV and other retroviruses lack a 3′-OH.

The other critical element in catalysis is the bound metal ion. Like all ATP-dependent kinases, NDP kinase takes a nucleotide–metal ion complex as substrate. Biochemical data indicate that the catalytic activity is very low unless a divalent ion is present, usually Mg^{2+} (Biondi *et al.*, 1998). The crystal structure of *Myxococcus* NDP kinase with metal-free ADP shows that Mg^{2+} is not required for binding, but the pyrophosphate moiety of ADP is disordered in its absence (Williams *et al.*, 1993). Cyclic AMP and PAPS also bind without metal, but these are inhibitors, not substrates. All other X-ray structures show a single Mg^{2+} ion ligating both the α- and the β-phosphate. In the ADP–BeF_3 and ADP–AlF_3 complexes, the Mg^{2+} ion also ligates one of the fluorides representing the γ-phosphate oxygens. The ion is octahedral and six-ligated in all cases, yet no protein group is directly involved, the six ligands being either phosphate oxygens or water molecules.

CONCLUSION

The catalysis of phosphate transfer by NDP kinase is very efficient and has many remarkable features. It

is an excellent example of substrate-assisted catalysis: the 3′-OH of the nucleotide sugar and the substrate bound Mg^{2+} are the two more important catalytic groups, except for the nucleophilic histidine. X-ray studies have shown that the mechanism and all major features except the quaternary structure are common to NDP kinases from many different sources. We should, therefore, expect to find the same subunit fold and mode of dimerization in all NDP kinases.

ACKNOWLEDGMENTS

This work was funded by Agence Nationale de la Recherche contre le SIDA and Association pour la Recherche contre le Cancer. YX acknowledges financial support by the France–China Programme de Recherches Avancées, PM, by Sidaction. We are grateful to Dr. Véron, Pr. Lascu, Dr. M.L. Lacombe, and their collaborators for the gift of many protein samples and a long-standing collaboration with our group.

REFERENCES

Adman, E. T., Sieker, L. C., and Jensen, L. H. (1973). *J. Biol. Chem.* **248**, 3987–3996.

Admiraal, S. J., Schneider, B., Meyer, P., Janin, J., Véron, M., Deville-Bonne, and Herschlag, D. (1999). *Biochemistry* **38**, 4701–4711.

Biggs, J., Hersperger, E., Steeg, P. S., Liotta, L. A., and Shearn, A. (1990). *Cell* **63**, 933–940.

Biondi, R. M., Schneider, B., Passeron, E., and Passeron, S. (1998). *Arch. Biochem. Biophys.* **353**, 85–92.

Bourdais, J., Biondi, R, Sarfati, S., Guerreiro, C., Lascu, I., Janin, J., and Véron, M. (1996). *J. Biol. Chem.* **271**, 7887–7890.

Bryant, S. H., Madej, T., Janin, J., Liu, Y., Ruoho, A. E., Zhang, G., and Hurley, H. (1997). *Nature (London)* **388**, 34.

Cherfils, J., Moréra, S., Lascu, I, Véron, M., and Janin, J. (1994). *Biochemistry* **33**, 9062–9069.

Chiadmi, M., Moréra, S., Lascu, I., Dumas, C., LeBras, G., Véron, M., and Janin, J. (1993). *Structure* **4**, 283–293.

De la Rosa, A., Williams, R. L., and Steeg, P. S. (1995). *Bioessays* **17**, 53–62.

Dumas, C., Lascu, I., Moréra, S., Glaser, P., Fourme, R., Wallet, V., Lacombe, M. L., Véron, M., and Janin, J. (1992) *EMBO J.* **11**, 3203–3208.

Giartoso, A., Erent, M., Cervoni, L., Moréra, S., Janin, J., Konrad, M., and Lascu, I. (1996). *J. Biol. Chem.* **271**, 17845–17851.

Gilles, A. M., Presecan, E., Vonica, A., and Lascu, L. (1991). *J. Biol. Chem.* **266**, 8784–8789.

Gonin, P., Xu, Y., Milon, L., Dabernat, S., Morr, M., Kumar, R., Lacombe, M. L., and Lascu, L. (1999). *Biochemistry* **38**, 7265–7272.

Herzberg, O., Reddy, P., Sutrina, S., Saier, M. H. J., Reizer, J., and Kapadia, P. (1992). *Proc. Nat. Acad. Sci. USA* **89**, 2499–2503.

Janin, J., Miller, S., and Chothia, C. (1988). *J. Mol. Biol.* **204**, 155–164.

Janin, J. (1993). *Nature* **365**, 21.

Karlsson, A., Mesnildrey, S., Xu, Y., Moréra, S., Janin, J., and Véron, M. (1996). *J. Biol. Chem.* **271**, 19928–19934.

Kinoshita, K., Sadanami, K., Kidera, A., and Go, N. (1999). *Protein Eng.* **12**, 11–14.

Ladher, J. E., Abdulaev, N. G., Kakuev, D. L., Tordova, M., Ridge, K. D., and Gilliland, G. L. (1999). *Acta Crystallog.* **D55**, 1127–1135.

Lascu, L., Chafotte, A., Limbourg-Bouchon, B., and Véron, M. (1992). *J. Biol. Chem.* **267**, 12775–12781.

Lecroisey, A., Lascu, L, Bominaar, A., Véron, M., and Delepierre, M. (1995). *Biochemistry* **34**, 12445–12450.

Meyer, P., Schneider, B., Sarfati, S., Deville-Bonne, D., Guerreiro, C., Boretto, J., Janin, J., Véron, M., and Canard, B. (2000). *Embod.* **19**, 3520–3529.

Milon, L., Rousseau-Merck, M. F., Munier, A., Erent, M., Lascu., I., Capeau, J., and Lacombe,M. L. (1997). *Human Genet.* **99**, 550–557.

Milon, L., Meyer, P., Chiadmi, M., Munier, A., Johansson, M., Karlsson, A., Lascu., I., Janin, J., Capeau, J., and Lacombe, M. L. (2000). *J. Biol. Chem.*, in press. Moodie, S. L., and Thornton, J. M. (1993). *Nucl. Acid Res.* **6**, 1369–1380.

Min, K., Kim, S. Y., Song, H. K., Chang, C., Cho, S. J., Moon, J., Yang, J. K., Lee, J. Y., Lee, K. J., and Suh, S. W. (2000). *Acta Crystallog.* **D56**, 504–505.

Moréra, S., LeBras, G., Lascu, I., Lacombe, M. L., Véron, M, and Janin, J. (1994a). *J. Mol. Biol.* **243**, 873–890.

Moréra, S., Lascu, I., Dumas, C., LeBras, G., Véron, M., and Janin, J. (1994b). *Biochemistry* **33**, 459–467.

Moréra, S., Chiadmi, M., LeBras, G., Lascu, I., and Janin, J. (1995a). *Biochemistry* **34**, 11062–11070.

Moréra, S., Lacombe, M. L., Xu, Y., LeBras, G., and Janin, J. (1995b). *Structure* **3**, 1307–1314.

Okabe-Kado, J., Kasukabe, T., Hozumi, M., Honma, Y., Kimura, N., Baba, H., Urano, T., and Shiku, H. (1995). *FEBS Lett.* **363**, 311–315.

Pastore, A., Saudek, V., Ramponi, G., and Williams, R. J. P. (1992). *J. Mol. Biol.* **224**, 427–440.

Postel, E. H. (1998). *Intern. J. Biochem. Cell Biol.* **30**, 1291–1295.

Schneider, B., Xu, Y., Sellam, O., Janin, J., Véron, M., and Deville-Bonne, D. (1998a). *J. Biol. Chem.* **273**, 28773–28778.

Schneider, B., Xu, Y., Sellam, O., Sarfati, R., Janin, J., Véron, M., and Deville-Bonne, D. (1998b). *J. Biol. Chem.* **273**, 11491–11497.

Schulz, G. E. (1992). *Current Opinion Struct. Biol.* **2**, 61–67.

Stahl, J. A., Leone, A., Rosengard, A. M., Porter, L., King, C. R. and Steeg, P. S. (1991). *Cancer Res.* **51**, 445–449.

Strelkov, S. V., Perisic, O., Webb, P. A., and Williams, R. L. (1995). *J. Mol. Biol.* **249**, 665–674.

Swindells, M. B., Orengo, C. A., Jones, D. T., Pearl, L. H., and Thornton, J. M. (1993). *Nature (London)* **365**, 21.

Swindells, M. B., and Alexandrov, N. N. (1994). *Nature Struct. Biol.* **1**, 677–678.

Tepper, A. D., Dammann, H., Bominaar, A. A., and Véron, M. (1994). *J. Biol. Chem.* **269**,1887–1890.

Webb, P. A., Perisic, O., Mendola, C. E., Backer, J. M., and Williams, R. L. (1995). *J. Mol. Biol.* **251**, 574–587.

Williams, R. L., Oren, D. A., Munoz-Dorado, J., Inouye, S., Inouye, M., and Arnold, E. (1993). *J. Mol. Biol.* **234**, 1230–1247.

Xiao, B., Shi, G., Chen, X., Yan, H., and Ji, X. (1999). *Structure* **7**, 489–496.

Xu, Y., Moréra, S., Janin, J., and Cherfils, J. (1997a). *Proc. Natl. Acad. Sci USA* **94**, 3579–3583.

Xu, Y., Sellam, O., Moréra, S., Sarfati, R., Véron, M., and Janin, J. (1997b). *Proc. Natl. Acad. Sci USA* **94**, 7162–7165.

Xu, Y., Lecroisey, Y., Véron, M., Delepierre, M., and Janin, J. (1997c). *Proteins* **28**, 150–152.